Supporting Information for

Cotton yield estimate using Sentinel-2 data and an ecosystem model over the Southern US

Submitted to ***MDPI Remote Sensing***

Liming He[1*] and Georgy Mostovoy[1]

[1]Laboratory of Environmental Model and Data Optima, Laurel, MD, USA, 20707

*Corresponding author: Liming He (liming.he@gmail.com; liming.he@emdous.com)

S1 Summary of the BEPS model structure

The Boreal Ecosystems Productivity Simulator (BEPS) - hourly version, is a process-based ecosystem model including water, energy and carbon budgets and soil thermal transfer modules (B. Z. Chen, J. M. Chen, & W. M. Ju, 2007; J. M. Chen, Liu, Cihlar, & Goulden, 1999; J. M. Chen et al., 2012; He, Chen, Liu, Bélair, & Luo, 2017; He et al., 2014). In this model, gross primary productivity (GPP) is modeled by scaling Farquhar's leaf-level biochemical model (Farquhar, Caemmerer, & Berry, 1980) up to the canopy level using a "two-leaf' approach (J. M. Chen et al., 1999; Norman, 1982). The bulk stomatal conductances of the sunlit and shaded leaves for water vapor and CO_2 are calculated using a modified Ball-Woodrow-Berry (BWB) stomatal model (Ball, Woodrow, & Beny, 1987). The Penman–Monteith equation (Monteith, 1965) is used to calculate the evaporation of intercepted water from the canopy and the ground surface, and canopy transpiration from sunlit and shaded leaves is computed following Y. P. Wang and Leuning (1998). The soil water dynamics is governed by the Richards equation (B. Chen, J. M. Chen, & W. Ju, 2007). The soil profile is stratified in five layers with depths of 0.05 m, 0.10 m, 0.20 m, 0.40 m, and 1.2 m from top layer to bottom layer. In BEPS, the influence of soil water on GPP is modeled through the modified BWB equation following G. B. Bonan (1995) and Weimin Ju et al. (2006).

Although BEPS was initially developed for boreal ecosystems, it has been expanded and used for temperate and tropical ecosystems in Asia (Matsushita & Tamura, 2002; Matsushita, Xu, Chen, Kameyama, & Tamura, 2004), China (Feng et al., 2007), Germany (Q. Wang et al., 2004), and other global applications (J. M. Chen et al., 2012; Z. Chen et al., 2017; He et al., 2018; He et al., 2017; Luo et al., 2018).

We summarize a few parts of BEPS that are related to the GPP modeling in detail below (He et al., 2014).

Supplementary Figure 1. (Fig. S1) A diagrammatic sketch for the BEPS model.

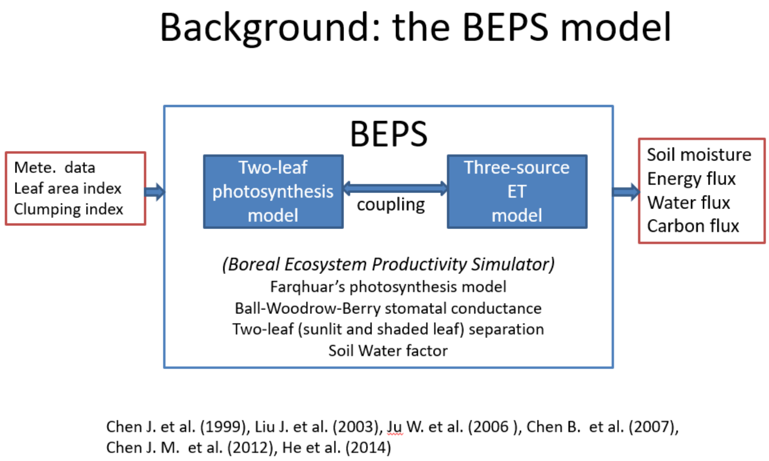

S2 Photosynthesis

The canopy-level photosynthesis (A_{canopy}) is simulated as the sum of the total photosynthesis of sunlit and shaded leaf groups (J. M. Chen et al., 1999):

$$A_{canopy} = A_{sun}(g_{sc\_sun})L_{sun} + A_{sh}(g_{sc\_sh})L_{sh} \quad (1)$$

where the subscripts "sun" and "sh" denote the sunlit and shaded components of the photosynthesis (*A*) and leaf area index (LAI, or *L*). g_{sc} is the stomatal resistance for carbon molecules. The sunlit and shaded LAI are separated by (J. M. Chen et al., 1999; Norman, 1982):

$$\begin{aligned} L_{sun} &= 2\cos\theta\left(1-e^{-0.5\Omega L/\cos\theta}\right) \\ L_{sh} &= L - L_{sun} \end{aligned} \quad (2)$$

where θ is the solar zenith angle, Ω is the clumping index.

The net rate of CO_2 assimilation (either A_{sun} or A_{sh}) is calculated as (Farquhar et al., 1980):

$$A = \min\left(A_c, A_j\right) - R_d \quad (3)$$

$$A_c = V_{c\max} f_V\left(T_l\right)\frac{C_i - \Gamma}{C_i + K_c\left(1 + O_i / K_o\right)} \quad (4)$$

$$A_j = \frac{I \cdot J_{\max} f_J\left(T_l\right)}{I + 2.1 J_{\max} f_J\left(T_l\right)} \cdot \frac{C_i - \Gamma}{4C_i + 8\Gamma} \quad (5)$$

where A, A_c, and A_j are the net photosynthetic, Rubisco-limited and light-limited gross photosynthetic rates μmol m^{-2} s^{-1}, respectively. R_d is the daytime leaf dark respiration, V_{cmax} is the maximum carboxylation rate at 25 °C ($V_{c\max,sun}$ and $V_{c\max,sh}$ for sunlit and shaded leaves, respectively). J_{max} is the electron transport rate at 25 °C. C_i and O_i are the intercellular CO_2 and oxygen concentration, respectively. Γ is the CO_2 compensation point without dark respiration, K_c and K_o are the Michaelis-Menten constants for CO_2 and oxygen respectively. I is the incident photosynthetically active photon flux (mmols m^{-2} s^{-1}). $f_V(T_l)$ and $f_J(T_l)$ are the leaf temperature (T_l) response functions for V_{cmax} and J_{max} respectively. In the model, the J_{max} is estimated from V_{cmax} (Medlyn et al., 1999):

$$J_{\max} = 2.39 \cdot V_{c\max} - 14.2 \quad (6)$$

In the current BEPS, $f_V(T_l)$ and $f_J(T_l)$ share the same formula:

$$f\left(Tl\right) = \frac{hkin \cdot e^{\frac{eakin \cdot \left(T_l - T_{opt}\right)}{rugc \cdot T_{opt} \cdot T_l}}}{hkin - eakin \cdot \left(1 - e^{\frac{hkin \cdot \left(T_l - T_{opt}\right)}{rugc \cdot T_{opt} \cdot T_l}}\right)} \quad (7)$$

Where, T_{opt} (301 K) is the optimum temperature for maximum carboxylation, and maximum electron transport, rugc (universal gas constant) = 8.314 J $mole^{-1}$ K^{-1}, hkin is the enthalpy term (200000.0 J mol^{-1}), eakin represents the activation energy for electron transport, or carboxylation (55000.0 J mol^{-1}).

S3 N-weighted V_{cmax} and J_{max} for sunlit and shaded leaves

The N-weighted V_{cmax} is derived according to J. M. Chen et al. (2012):

$$V_{c\max,sun} = V_{c\max,0} \chi_n N_0 \frac{k\left[1 - \mathrm{e}^{-(k_n + k)L}\right]}{\left(k_n + k\right)\left(1 - e^{-kL}\right)}$$

$$V_{c\max,sh} = V_{c\max,0} \chi_n N_0 \frac{\frac{1}{k_n}\left(1 - e^{-k_n L}\right) - \left(1 - \mathrm{e}^{-(k_n + k)L}\right)\frac{\Omega}{\left(k_n + k\right)}}{L - 2\cos\theta\left(1 - e^{-kL}\right)} \quad (8)$$

where $V_{cmax,0}$ is the leaf maximum Rubisco capacity at the top of the canopy at 25°C, χ_n is the ratio of measured Rubisco capacity to leaf N (Dai, Dickinson, & Wang, 2004; dePury & Farquhar, 1997), N_0 is the N content at the top of the canopy; $k = G(\theta)\Omega / \cos\theta$, $G(\theta)$ is the projection coefficient, usually taken as 0.5 for spherical leaf angle distribution, k_n is the leaf N content decay rate with increasing depth into the canopy, taken as equal to 0.3 after dePury and Farquhar (1997).

S4 Surface evaporation and Canopy level transpiration

The latent heat (LE) is simulated as:

$$LE = \lambda\left(T + E_l + E_g\right) \tag{9}$$

where λ is the latent heat of vaporization. T is the transpiration rate from canopy (kg m^{-2} s^{-1}), E_l and E_g are evaporation rates of intercepted water from canopy and ground surface (kg m^{-2} s^{-1}), respectively.

The canopy level transpiration is obtained by:

$$T = T_{sun}(g_{s\_sun})L_{sun} + T_{sh}(g_{s\_sh})L_{sh} \tag{10}$$

where T_{sun} and T_{sh} are the average transpiration rates for sunlit and shaded leaves, respectively. The nonlinear relationship between T_{sun} (T_{sh}) and L_{sun} (L_{sh}) is considered in the parameters used to calculate T. g_s is stomatal resistance for water molecules. g_s/g_{sc} =1.6. Following Y. P. Wang and Leuning (1998), transpiration from sunlit leave is calculated as (W. Ju, Wang, Yu, Zhou, & Wang, 2010):

$$T_{sun} = \frac{D_a + \Delta\left(T_{s,sun} - T_a\right)}{r_{sun}} \frac{\rho C_p}{\gamma} \tag{11}$$

where D_a is the atmospheric vapor pressure deficit (kPa). Δ is the rate of change of the saturated vapor pressure with temperature (kPa °C^{-1}). $T_{s,sun}$ and T_a are temperatures at sunlit leaf surface and air temperature (°C), respectively. ρ is the air density (kg m^{-3}). C_p is the specific heat of air at constant temperature (1010 Jkg^{-1}°C^{-1}), and

$$r_{sun} = r_b + r_a + 1/g_{s\_sun} \tag{12}$$

where r_a and r_b are aerodynamic and boundary layer resistance (s m^{-1}), respectively, and γ is the psychrometric constant (kPa °C^{-1}). To calculate T_{sh}, $T_{s,sh}$ (temperature at shaded leaf surface) and g_{s_sh} are used to replace $T_{s,sun}$ and g_{s_sun} in eq. (11) and (12).

The evaporation from soil E_g is estimated using the Penman–Monteith equation (Monteith, 1965):

$$\lambda E_g = \frac{\Delta\left(R_g - 0\right) + \rho C_p VPD\_g / \mathrm{r}_{\mathrm{a\_g}}}{\Delta + \gamma\left(1 + \mathrm{r}_{\mathrm{soil}} / r_{a\_g}\right)} \tag{13}$$

where R_g is the net radiation in the ground, VPD_g is Vapor pressure deficit at the ground level, r_{a_g} is the aerodynamic resistance of ground surface, r_{soil} is the soil resistance for evaporation. In Sellers et al. (1996),

$$\mathrm{r}_{\mathrm{soil}} = \exp\left(8.2 - 4.2 \cdot \theta_1 / \theta_s\right) \tag{14}$$

where θ_1 is volumetric soil VWC in first layer (m^3 m^{-3}), and θ_s is value of θ at saturation (m^3 m^{-3}). The r_{soil} from Sellers et al. (1996) is a rough estimate that is derived from bare soil surface (Sellers, Heiser, & Hall, 1992). The evaporation can be overestimated if this equation is used since it does not consider the organic layer in the soil horizons. In BEPS, we used 4* r_{soil} in the BEPS model.

The evaporation from intercepted water from sunlit and shaded leave E_l are estimated similarly using eq. (13) to (14), but without the term for stomatal resistance (i.e., r_s=0).

S5 Simulation of stomatal closure with rising CO_2 concentration in BEPS.

Leaf stomata control the exchanges of water vapor and CO_2 between plants and the atmosphere. Under high atmospheric CO_2 concentration, stomatal density and hence conductance may decrease (Franks & Beerling, 2009). BEPS inherits the Ball-Woodrow-Berry (BWB) equation to model stomatal conductance (g_s, µmol m^{-2} s^{-1}) (Ball et al., 1987):

$$g_s = g_0 + m \cdot h_s \cdot p \cdot \frac{A}{C_s} \tag{15}$$

where g_0 is a small value, the stomatal conductance at the light compensation point, m is a plant species dependent coefficient, h_s is the relative humidity at the leaf surface, p is the atmospheric pressure, A is the photosynthesis rate, and C_s is the molar fraction of CO_2 at the leaf surface.

The important influences of soil water on *g* and *A* are not mechanistically included in the original BWB formulation. Following G. B. Bonan (1995) and Weimin Ju et al. (2006), we modify it as follows:

$$g_s = g_0 + f_w \cdot m \cdot h_s \cdot p \cdot \frac{A}{C_s} \tag{16}$$

where f_w is a soil water stress factor, which we assume to be a function of soil water content.

In Weimin Ju et al. (2006), the fw is modeled as:

$$f_w = \sum_{i=1}^{n} f_{w,i} w_i \tag{17}$$

where *fw,i* is the soil water availability factor in layer *i*, and calculated as:

$$f_{w,i} = \frac{1.0}{f_i(\psi_i) f_i(T_{s,i})} \tag{18}$$

where $f_i(\psi_i)$ is a function of matrix suction ψ_i(m) (Zierl, 2001):

$$f_i(\psi_i) = \begin{cases} 1.0 + \left[\dfrac{\psi_i - 10.0}{10.0}\right]^{\alpha} ? & \psi_i > 10 \\ 1.0? & else \end{cases} \tag{19}$$

where α is suggested to be a function of plant type (J. M. Chen et al., 2012).

The effect of soil temperature on soil water uptake is described as follows (Gordon B. Bonan, 1991):

$$f_i(T_{s,i}) = \begin{cases} \dfrac{1.0}{1 - \exp\left(t_1 {T^{t_2}}_{s,i}\right)} & T_{s,i} > 0 \\ \infty & else \end{cases} \tag{20}$$

where t_1 and t_2 are two parameters determining the sensitivity of water uptake by roots to soil temperature. In the BEPS, t_1 = -0.02 and t_2 = 2.0.

To consider the variable soil water potential at different depths, w_i is calculated as:

$$w_i = \frac{R_i f_{w,i}}{\sum_{i=1}^{n} R_i f_{w,i}} \quad (21)$$

where R_i is the root fraction in layer *i*.

Apparently, g_s will increase with *A* (due to increase in photosynthetically active radiation (PAR) and / or V_{cmax}) assuming there is no change in f_w , *m*, h_s, *p*, and C_s.

The BWB equation can simulate the stomatal closure due to CO_2 fertilization. Assuming that there is no change in f_w , *m*, h_s, *p*, V_{cmax} and PAR, there is an associated increase in intercellular CO_2 concentration (C_i) for an increase in C_s. Since *A* is often limited either by Rubisco or by Electron-transport rate, the increase in *A* will be not proportional to C_s; or in other words, the ratio of *A* to C_s will remain the same or decrease with rising C_s. As a result, the g_s in the left side of BWB equation will remain the same or decrease (leading to stomatal closure) with rising C_s (Baldocchi, 1994).

The BWB equation is used in many climate models, such as those in Coupled Model Intercomparison Project Phase 5 (CMIP5, http://www.nature.com/ngeo/journal/v6/n6/fig_tab/ngeo1801_T1.html) and TRENDY (Sitch et al., 2008) to study the global transpiration decrease (or increase of water use efficiency) due to CO_2 fertilization (Frank et al., 2015; Swann, Hoffman, Koven, & Randerson, 2016).

S6 Calculations of radiation at Sunlit- and Shaded- leaf groups

We refer to "Appendix A. Algorithms for net radiation of vegetation and ground surface" by B. Chen et al. (2016) for radiation calculation.

S7 Calculations of Sunlit- and Shaded- leaf temperatures

For a sunlit or shaded leaf, its temperature (T_l) is calculated as below during an iteration.

$$T_l = T_a + \frac{R_n - VPD_a \cdot \rho_a \cdot Cp_{ca} \cdot p^*}{\rho_a \cdot Cp_{ca} \cdot (G_h + \Delta \cdot p^*)} \quad (22)$$

where, T_a is the air temperature in °C, R_n is the net radiation of sunlit- or shaded- leaf calculated from S1.6, VPD_a is water vapor deficit at the reference height, ρ_a is the density of air at 0 °C, Cp_{ca} is specific heat of moist air above the canopy, G_h is the total conductance for heat transfer from the leaf surface to the reference height above the canopy, Δ is the rate of change (slope) of the saturated vapor pressure with temperature (kPa °C^{-1}),

$$p^* = \frac{G_w + G_{ww} \cdot \left(X_{cs} + X_{cl} \right)}{psychrometer} \tag{23}$$

where, G_w is the total conductance for water from the intercellular space of the leaves to the reference height above the canopy, G_{ww} is the total conductance for water from the surface of the leaves to the reference height above the canopy, Psychrometer is the psychrometric constant (0.066), X_{cl} and X_{cs} are the fractions of canopy covered by liquid water and snow.

S8 Forcing data and model parameters.

Climate reanalysis data are the outputs of an Earth system model that assimilates various archived observations. Global reanalysis data are the best available datasets for this study. MERRA-2 (Modern-Era Retrospective Analysis for research and Applications, Version 2) data from GSFC, NASA are used to drive BEPS to simulate GPP and ET in 2017 (Rienecker et al., 2011). The data have a spatial resolution of 0.625° (longitude) by 0.5° (latitude) and a temporal resolution of one hour. To drive BEPS, relative humidity, wind speed, and air temperature at 2 m above the surface, surface atmosphere pressure and incoming solar shortwave flux, and total precipitation at the surface level are spatially interpolated to the 20 m grid. The precipitation data from MERRA are corrected by global gauge-based NOAA Climate Prediction Center "Unified" (CPCU) precipitation product (CPCU). Recent validation suggests that MERRA2 datasets have relative small errors comparing to a few other reanalysis datasets (Draper, Reichle, & Koster, 2018; Eyre & Zeng, 2017; Reichle, Draper, et al., 2017; Reichle, Liu, et al., 2017; Simmons et al., 2017).

To simulate the CO2 fertilization effect, the CO2 concentration data are from https://www.esrl.noaa.gov/gmd/ccgg/trends/global.html.

S9 Previous validations of BEPS

Recent validations of GPP against eddy covariance measurements suggest that BEPS can explain more than 80% of the daily GPP variance at flux tower sites (Gonsamo et al., 2013; Sprintsin, Chen, Desai, & Gough, 2012). When soil water stress is properly addressed, BEPS explains 56-90% of the hourly GPP variance for maximum LAI values ranging from 2.1 to 8 (B. Chen et al., 2016). In 2018, the BEPS-simulated GPP is validated against eddy covariance measurements from 124 flux tower sites (FLUXNET2015 Dataset in Tier 1; http://fluxnet.fluxdata.org/) at the site level; validation suggests that BEPS simulates annual GPP well with a coefficient of determinations (R^2) of 0.81, a RMSE of 347 g C m^{-2} yr^{-1}, and a bias of 172 g C m^{-2} yr^{-1} (He et al., 2018).

Baldocchi, D. (1994). An Analytical Solution for Coupled Leaf Photosynthesis and Stomatal Conductance Models. *Tree Physiology, 14*(7-9), 1069-1079.

Ball, J., Woodrow, L. E., & Beny, J. A. (1987). A model predicting stomatal conductance and its contribution to the control of photosynthesis under different environmental conditions. In J. Biggins (Ed.), *Progress in Photosynthesis research* (Vol. 4, pp. 221-224): Nijhoff, Dordrecht.

Bonan, G. B. (1991). A biophysical surface energy budget analysis of soil temperature in the boreal forests of interior Alaska. *Water Resources Research, 27*(5), 767-781. doi:10.1029/91WR00143

Bonan, G. B. (1995). Land Atmosphere Co2 Exchange Simulated by a Land-Surface Process Model Coupled to an Atmospheric General-Circulation Model. *Journal of Geophysical Research-Atmospheres, 100*(D2), 2817-2831. doi:Doi 10.1029/94jd02961

Chen, B., Chen, J. M., & Ju, W. (2007). Remote sensing-based ecosystem–atmosphere simulation scheme (EASS)—Model formulation and test with multiple-year data. *Ecological Modelling, 209*(2–4), 277-300. doi:http://dx.doi.org/10.1016/j.ecolmodel.2007.06.032

Chen, B., Liu, J., Chen, J. M., Croft, H., Gonsamo, A., He, L., & Luo, X. (2016). Assessment of foliage clumping effects on evapotranspiration estimates in forested ecosystems. *Agricultural and Forest Meteorology, 216*, 82-92. doi:http://dx.doi.org/10.1016/j.agrformet.2015.09.017

Chen, B. Z., Chen, J. M., & Ju, W. M. (2007). Remote sensing-based ecosystem-atmosphere simulation scheme (EASS) - Model formulation and test with multiple-year data. *Ecological Modelling, 209*(2-4), 277-300. doi:DOI 10.1016/j.ecolmodel.2007.06.032

Chen, J. M., Liu, J., Cihlar, J., & Goulden, M. L. (1999). Daily canopy photosynthesis model through temporal and spatial scaling for remote sensing applications. *Ecological Modelling, 124*(2-3), 99-119. doi:Doi 10.1016/S0304-3800(99)00156-8

Chen, J. M., Mo, G., Pisek, J., Liu, J., Deng, F., Ishizawa, M., & Chan, D. (2012). Effects of foliage clumping on the estimation of global terrestrial gross primary productivity. *Global Biogeochemical Cycles, 26*. doi:Artn Gb1019. Doi 10.1029/2010gb003996

Chen, Z., Chen, J. M., Zhang, S., Zheng, X., Ju, W., Mo, G., & Lu, X. (2017). Optimization of terrestrial ecosystem model parameters using atmospheric CO2 concentration data with the Global Carbon Assimilation System (GCAS). *Journal of Geophysical Research: Biogeosciences*, n/a-n/a. doi:10.1002/2016JG003716

Dai, Y. J., Dickinson, R. E., & Wang, Y. P. (2004). A two-big-leaf model for canopy temperature, photosynthesis, and stomatal conductance. *Journal of Climate, 17*(12), 2281-2299. doi:Doi 10.1175/1520-0442(2004)017<2281:Atmfct>2.0.Co;2

dePury, D. G. G., & Farquhar, G. D. (1997). Simple scaling of photosynthesis from leaves to canopies without the errors of big-leaf models. *Plant Cell and Environment, 20*(5), 537-557. doi:DOI 10.1111/j.1365-3040.1997.00094.x

Draper, C. S., Reichle, R. H., & Koster, R. D. (2018). Assessment of MERRA-2 Land Surface Energy Flux Estimates. *Journal of Climate, 31*(2), 671-691.

Eyre, J. E. J. R., & Zeng, X. B. (2017). Evaluation of Greenland near surface air temperature datasets. *Cryosphere, 11*(4), 1591-1605.

Farquhar, G. D., Caemmerer, S. V., & Berry, J. A. (1980). A Biochemical-Model of Photosynthetic Co2 Assimilation in Leaves of C-3 Species. *Planta, 149*(1), 78-90. doi:Doi 10.1007/Bf00386231

Feng, X., Liu, G., Chen, J. M., Chen, M., Liu, J., Ju, W. M., . . . Zhou, W. (2007). Net primary productivity of China's terrestrial ecosystems from a process model driven by remote sensing. *Journal of Environmental Management, 85*(3), 563-573.

Frank, D. C., Poulter, B., Saurer, M., Esper, J., Huntingford, C., Helle, G., . . . Weigl, M. (2015). Water-use efficiency and transpiration across European forests during the Anthropocene. *Nature Climate Change, 5*(6), 579-+.

Franks, P. J., & Beerling, D. J. (2009). Maximum leaf conductance driven by CO2 effects on stomatal size and density over geologic time. *Proceedings of the National Academy of Sciences of the United States of America, 106*(25), 10343-10347. doi:10.1073/pnas.0904209106

Gonsamo, A., Chen, J. M., Price, D. T., Kurz, W. A., Liu, J., Boisvenue, C., . . . Chang, K. H. (2013). Improved assessment of gross and net primary productivity of Canada's landmass. *Journal of Geophysical Research-Biogeosciences, 118*(4), 1546-1560. doi:10.1002/2013jg002388

He, L., Chen, J. M., Gonsamo, A., Luo, X. Z., Wang, R., Liu, Y., & Liu, R. G. (2018). Changes in the Shadow: The Shifting Role of Shaded Leaves in Global Carbon and Water Cycles Under Climate Change. *Geophysical Research Letters, 45*(10), 5052-5061.

He, L., Chen, J. M., Liu, J., Bélair, S., & Luo, X. (2017). Assessment of SMAP soil moisture for global simulation of gross primary production. *Journal of Geophysical Research: Biogeosciences, 122*, doi:10.1002/2016JG003603. doi:10.1002/2016JG003603

He, L., Chen, J. M., Liu, J., Mo, G., Bélair, S., Zheng, T., . . . Barr, A. G. (2014). Optimization of water uptake and photosynthetic parameters in an ecosystem model using tower flux data. *Ecological Modelling, 294*(0), 94-104. doi:http://dx.doi.org/10.1016/j.ecolmodel.2014.09.019

Ju, W., Chen, J. M., Black, T. A., Barr, A. G., Liu, J., & Chen, B. (2006). Modelling multi-year coupled carbon and water fluxes in a boreal aspen forest. *Agricultural and Forest Meteorology, 140*(1-4), 136-151. doi:10.1016/j.agrformet.2006.08.008

Ju, W., Wang, S., Yu, G., Zhou, Y., & Wang, H. (2010). Modeling the impact of drought on canopy carbon and water fluxes for a subtropical evergreen coniferous plantation in southern China through parameter optimization using an ensemble Kalman filter. *Biogeosciences, 7*(3), 845-857.

Luo, X. Z., Chen, J. M., Liu, J. E., Black, T. A., Croft, H., Staebler, R., . . . McCaughey, H. (2018). Comparison of Big-Leaf, Two-Big-Leaf, and Two-Leaf Upscaling Schemes for Evapotranspiration Estimation Using Coupled Carbon-Water Modeling. *Journal of Geophysical Research-Biogeosciences, 123*(1), 207-225. doi:10.1002/2017jg003978

Matsushita, B., & Tamura, M. (2002). Integrating remotely sensed data with an ecosystem model to estimate net primary productivity in East Asia. *Remote Sensing of Environment, 81*(1), 58-66.

Matsushita, B., Xu, M., Chen, J., Kameyama, S., & Tamura, M. (2004). Estimation of regional net primary productivity (NPP) using a process-based ecosystem model: How important is the accuracy of climate data? *Ecological Modelling, 178*(3-4), 371-388.

Medlyn, B. E., Badeck, F. W., De Pury, D. G. G., Barton, C. V. M., Broadmeadow, M., Ceulemans, R., . . . Jarvis, P. G. (1999). Effects of elevated [CO2] on photosynthesis in European forest species: a meta-analysis of model parameters. *Plant Cell and Environment, 22*(12), 1475-1495. doi:DOI 10.1046/j.1365-3040.1999.00523.x

Monteith, J. L. (1965). Evaporation and environment. *Symposia of the Society for Experimental Biology, 19*, 205-224.

Norman, J. M. (1982). SIMULATION OF MICROCLIMATES. In H. Jerry (Ed.), *Biometeorology in Integrated Pest Management* (pp. 65-99): Academic Press.

Reichle, R. H., Draper, C. S., Liu, Q., Girotto, M., Mahanama, S. P. P., Koster, R. D., & De Lannoy, G. J. M. (2017). Assessment of MERRA-2 Land Surface Hydrology Estimates. *Journal of Climate, 30*(8), 2937-2960.

Reichle, R. H., Liu, Q., Koster, R. D., Draper, C. S., Mahanama, S. P. P., & Partyka, G. S. (2017). Land Surface Precipitation in MERRA-2. *Journal of Climate, 30*(5), 1643-1664.

Rienecker, M. M., Suarez, M. J., Gelaro, R., Todling, R., Bacmeister, J., Liu, E., . . . Woollen, J. (2011). MERRA: NASA's Modern-Era Retrospective Analysis for Research and Applications. *Journal of Climate, 24*(14), 3624-3648.

Sellers, P. J., Heiser, M. D., & Hall, F. G. (1992). Relations between Surface Conductance and Spectral Vegetation Indexes at Intermediate (100m2 to 15km2) Length Scales. *Journal of Geophysical Research-Atmospheres, 97*(D17), 19033-19059.

Sellers, P. J., Randall, D. A., Collatz, G. J., Berry, J. A., Field, C. B., Dazlich, D. A., . . . Bounoua, L. (1996). A revised land surface parameterization (SiB2) for atmospheric GCMs .1. Model formulation. *Journal of Climate, 9*(4), 676-705. doi:Doi 10.1175/1520-0442(1996)009<0676:Arlspf>2.0.Co;2

Simmons, A. J., Berrisford, P., Dee, D. P., Hersbach, H., Hirahara, S., & Thepaut, J. N. (2017). A reassessment of temperature variations and trends from global reanalyses and monthly surface climatological datasets. *Quarterly Journal of the Royal Meteorological Society, 143*(702), 101-119.

Sitch, S., Huntingford, C., Gedney, N., Levy, P. E., Lomas, M., Piao, S. L., . . . Woodward, F. I. (2008). Evaluation of the terrestrial carbon cycle, future plant geography and climate-carbon cycle feedbacks using five Dynamic Global Vegetation Models (DGVMs). *Global Change Biology, 14*(9), 2015-2039.

Sprintsin, M., Chen, J. M., Desai, A., & Gough, C. M. (2012). Evaluation of leaf-to-canopy upscaling methodologies against carbon flux data in North America. *Journal of Geophysical Research-Biogeosciences, 117*. doi:Artn G01023

10.1029/2010jg001407

Swann, A. L. S., Hoffman, F. M., Koven, C. D., & Randerson, J. T. (2016). Plant responses to increasing CO2 reduce estimates of climate impacts on drought severity. *Proceedings of the National Academy of Sciences of the United States of America, 113*(36), 10019-10024.

Wang, Q., Tenhunen, J., Falge, E., Bernhofer, C., Granier, A., & Vesala, T. (2004). Simulation and scaling of temporal variation in gross primary production for coniferous and deciduous temperate forests. *Global Change Biology, 10*(1), 37-51.

Wang, Y. P., & Leuning, R. (1998). A two-leaf model for canopy conductance, photosynthesis and partitioning of available energy I: Model description and comparison with a multi-layered model. *Agricultural and Forest Meteorology, 91*(1-2), 89-111. doi:Doi 10.1016/S0168-1923(98)00061-6

Zierl, B. (2001). A water balance model to simulate drought in forested ecosystems and its application to the entire forested area in Switzerland. *Journal of Hydrology, 242*(1-2), 115-136.